Earth and Planetary Science Letters 333–334 (2012) 293–303

Contents lists available at SciVerse ScienceDirect

Earth and Planetary Science Letters

journal homepage: www.elsevier.com/locate/epsl

Timing and origin of recent regional ice-mass loss in Greenland

Ingo Sasgen [a,*], Michiel van den Broeke [b], Jonathan L. Bamber [c], Eric Rignot [d,e], Louise Sandberg Sørensen [f], Bert Wouters [g], Zdeněk Martinec [h], Isabella Velicogna [d,e], Sebastian B. Simonsen [i,j]

[a] Department of Geodesy and Remote Sensing, GFZ German Research Centre for Geosciences, Telegrafenberg A20, D-14473 Potsdam, Germany
[b] Institute for Marine and Atmospheric Research, Utrecht University, 3508 TA Utrecht, The Netherlands
[c] School of Geographical Sciences, University of Bristol, University Road, Bristol BS8 1SS, United Kingdom
[d] Jet Propulsion Laboratory, California Institute of Technology, Mail Stop 300-319, Pasadena, CA 91109-8099, USA
[e] Department of Earth System Science, University of California Irvine, CA 92697, USA
[f] National Space Institute, Technical University of Denmark, Juliane Maries Vej 30, 2100 Copenhagen, Denmark
[g] Royal Netherlands Meteorological Institute, Wilhelminalaan 10, NL-3732 GK De Bilt, The Netherlands
[h] School of Theoretical Physics, Dublin Institute for Advanced Studies, 10 Burlington Road, Dublin 4, Ireland
[i] Centre for Ice and Climate, Niels Bohr Institute, University of Copenhagen, Juliane Maries Vej 30, 2100 Copenhagen, Denmark
[j] Danish Climate Centre, DMI, Lyngbyvej 100, 2100 Copenhagen, Denmark

ARTICLE INFO

Article history:
Received 23 August 2011
Received in revised form
27 March 2012
Accepted 29 March 2012
Editor: T. Spohn
Available online 24 May 2012

Keywords:
mass balance
Greenland
GRACE
InSAR
RACMO
ICESat

ABSTRACT

Within the last decade, the Greenland ice sheet (GrIS) and its surroundings have experienced record high surface temperatures (Mote, 2007; Box et al., 2010), ice sheet melt extent (Fettweis et al., 2011) and record-low summer sea-ice extent (Nghiem et al., 2007). Using three independent data sets, we derive, for the first time, consistent ice-mass trends and temporal variations within seven major drainage basins from gravity fields from the Gravity Recovery and Climate Experiment (GRACE; Tapley et al., 2004), surface-ice velocities from Inteferometric Synthetic Aperture Radar (InSAR; Rignot and Kanagaratnam, 2006) together with output of the regional atmospheric climate modelling (RACMO2/GR; Ettema et al., 2009), and surface-elevation changes from the Ice, cloud and land elevation satellite (ICESat; Sørensen et al., 2011). We show that changing ice discharge (D), surface melting and subsequent run-off (M/R) and precipitation (P) all contribute, in a complex and regionally variable interplay, to the increasingly negative mass balance of the GrIS observed within the last decade. Interannual variability in P along the northwest and west coasts of the GrIS largely explains the apparent regional mass loss increase during 2002–2010, and obscures increasing M/R and D since the 1990s. In winter 2002/2003 and 2008/2009, accumulation anomalies in the east and southeast temporarily outweighed the losses by M/R and D that prevailed during 2003–2008, and after summer 2010. Overall, for all basins of the GrIS, the decadal variability of anomalies in P, M/R and D between 1958 and 2010 (w.r.t. 1961–1990) was significantly exceeded by the regional trends observed during the GRACE period (2002–2011).

1. Introduction

The GrIS is an important part of the climate system that interacts with other components in many ways, including the discharge of freshwater by surface melting and iceberg calving, changing sea-level and potentially affects the ocean's thermohaline circulation. Satellite observations have led to a general consensus about the increasingly negative mass balance for the GrIS since the late 1990s (e.g. Krabill et al., 2004; Cazenave, 2006; Hanna et al., 2005; Thomas et al., 2006; Zwally and Giovinetto, 2011), with a significant contribution of $\sim 0.7 \pm 0.1$ mm/yr (2003–2008; van den Broeke et al., 2009) to the observed global sea level rise of 3.1 ± 0.6 mm/yr (1993–2008; Ablain et al., 2009). A negative ice sheet mass balance means that the amount of mass gained by surface accumulation through rain and snow (P) is smaller than that lost by ablation, i.e. the combined effect of melting and subsequent meltwater run-off (M/R) and sublimation (SU), as well as ice discharge across the grounding line (D). The difference of P–SU–R approximates the surface-mass balance (SMB) neglecting snowdrift sublimation ($<6\%$ of SMB; Ettema et al., 2009), SMB–D represents the mass balance of the ice sheet, whereas the time integrated (i.e. cumulative) SMB and D anomalies (here, w.r.t. 1961–1990) represent change in mass stored by the ice sheet, that are measured by GRACE and ICESat.

* Corresponding author. Tel.: +49 331 288 1145; fax: +49 331 288 1163.
E-mail address: sasgen@gfz-potsdam.de (I. Sasgen).

0012-821X/$ - see front matter © 2012 Elsevier B.V. All rights reserved.
http://dx.doi.org/10.1016/j.epsl.2012.03.033

For the GrIS, abrupt changes in ice motion have locally been linked to penetration of surface meltwater to the bed (Zwally et al., 2002; Bartholomew et al., 2010). For individual marine-terminating glaciers, intruding warm ocean waters have been identified as a cause for enhanced submarine melting that leads to the thinning or disintegration of floating ice tongues and grounding line retreat, with a resultant increase in discharge (Rignot et al., 2010; Holland et al., 2010). Regional atmospheric climate models supported by passive microwave data indicate a changing ratio between surface melt and precipitation, leading to an increasing imbalance between accumulation and ablation over the last two decades (Fettweis et al., 2011). Enhanced meltwater production is consistent with a general warming of the Arctic atmosphere in the past 30 yr (Mote, 2007; Hanna et al., 2008).

Here, we derive regional mass variations of the GrIS using three methods: (i) measuring variations in the Earth's gravitational potential with GRACE, (ii) contrasting SMB from the regional atmospheric climate model RACMO2/GR (Ettema et al., 2009) with D over the grounding line from InSAR (hereafter SMB–D), and (iii) determining surface elevation changes with the Geoscience Laser Altimeter System on ICESat. Each method has its strengths and weaknesses; e.g. ICESat altimetry measurements are accurate, but yield geometric volume changes that need to be converted to mass changes, relying on the accuracy of a snow/ice density model. SMB–D gives the best physical insight into the processes driving mass change, but it relies on subtracting two large numbers, where uncertainties of the difference can be significant w.r.t. SMB or D. In this respect, GRACE is advantageous, because it provides at regular (sub-)monthly intervals the gravity field disturbances induced by net ice-mass changes. However, the GRACE resolution of ~ 400 km is much coarser than that of ICESat (track-spacing < 30 km for GrIS) or the regional climate model RACMO2/GR (11 km). Also, GRACE is influenced by all mass changes in the Earth system, ranging from short-term atmospheric pressure variations to the long-term redistribution of mantle material caused by the glacial-isostatic adjustment (GIA). Despite these limitation, van den Broeke et al. (2009) and Rignot et al. (2011) have demonstrated a promising agreement of SMB–D with GRACE for mass trends of the entire GrIS, which are also consistent with ICESat (Sørensen et al., 2011). As shown below, we find excellent basin-scale agreement of the temporal mass variations of GrIS from GRACE and SMB–D, and trends from ICESat, allowing us, for the first time, to provide a robust regional separation of the relative importance of P, M/R and D in causing recent GrIS mass loss.

2. Data sets and methods

2.1. GRACE

In this study, 103 unconstrained monthly mean GRACE gravity field solutions of the Centre for Space Research at University of Texas, Austin, USA (CSR RL04; Bettadpur, 2007) were used, covering the time period from August 2002 to September 2011. The solutions of CSR RL04, available from http://isdc.gfz-potsdam.de/, are represented as Stokes potential coefficients complete to spherical-harmonic degree and order 60. During post-processing of the GRACE data, each monthly set of Stokes coefficients is smoothed with an isotropic spatial averaging function (Sasgen et al., 2006), which optimizes the trade-off between spatial resolution – typically between 400 and 500 km – and noise with respect to the expected signals. For further regionalization, the weight of low degree and order coefficients are reduced according to the correlation of predicted GrIS mass signal (from ICESat) and its superposition with GIA in response to the history of the Laurentide ice sheet. The band-pass filtered gravity fields are corrected for GIA and simultaneously inverted for monthly mean mass anomalies within seven major GrIS drainage basins and Ellesmere Island with a forward modeling approach (Appendix A1). The uncertainty associated with the filtering and inversion procedure for the entire GrIS was estimated to be 75 mm equivalent water height for the monthly solutions and about $\pm 7\%$ for the linear trends (Appendix A2). Following Paulson et al. (2007), the GIA correction is a version of ICE-5G (Peltier, 2004), adjusted to reconcile with the GRACE estimates, assuming upper- and lower-mantle viscosities of 6×10^{20} Pa s and 2×10^{22} Pa s (Wolf et al., 2004), and an elastic lithosphere with a thickness of 100 km. The uncertainty of the GIA corrections is assessed with the alternative retreat history of Lambeck and Chappell (2001), and by varying upper- and lower-mantle viscosities between 2×10^{20} and 8×10^{20} Pa s and between 5×10^{21} and 4×10^{22} Pa s, respectively, and the thickness of the lithosphere by ± 20 km. Depending on the applied GIA scenario (i.e. load history and viscosity distributions), GrIS mass loss presented here could be stronger by -3 Gt/yr or weaker by 20 Gt/yr (Table 1 and Appendix A3); this uncertainty agrees with the range (difference between minimum and maximum correction) of 29 ± 6 Gt/yr provided in the more complete GIA assessment of Barletta et al. (2008).

2.2. SMB–D

The surface mass balance (SMB) estimate is obtained from the regional climate model RACMO2/GR (Ettema et al., 2009) providing monthly means of the individual SMB components, i.e. precipitation, evaporation/sublimation, run-off, melting and re-freezing. The model is forced at its lateral boundaries and at the sea surface with atmospheric reanalysis data of the European Centre for Medium-Range Weather Forecasts (ECMWF) and run at a spatial resolution of ~ 11 km. Due to unavailability of data, our SMB time series is 1 yr shorter than that of GRACE, ending August 2010. The uncertainty of the SMB provided by RACMO2/GR is estimated to be $\pm 18\%$ (Ettema et al., 2009). It should be noted that RACMO2/GR and other regional climate models, e.g. MAR (Fettweis et al., 2011), Polar MM5 (Box et al., 2004), or ECMWF reanalysis (Hanna et al., 2011), may differ considerably in the absolute values provided for P and M/R; the temporal behaviour, however, is captured by all models, and the uncertainty is considerably reduced by building anomalies w.r.t. the reference period 1961–1990, as we will do in the following. The discharge (D) estimate is based on InSAR satellite observations of ice flow within 38 drainage basins (Rignot and Kanagaratnam, 2006) using the speckle tracking method, updated until the year 2009; due to unavailability of data, D is assumed to remain unchanged in 2010, compared to 2009. Ice-velocity is measured at flux gates located upstream of the grounding line and therefore a SMB estimate based on RACMO2/GR for the region located in between is added to the measurement at the flux gates. Together with ice thickness

Table 1
Regional mass trends of the GrIS from GRACE, SMB–D and ICESat for the common time interval October 2003–2009. The GRACE results are provided for CSR RL04 and two GIA corrections, ICE-5G* and ANU* (Appendix A3).

Drainage basin	Area (10^3 km^2)	GRACE (CSR RL04)		SMB–D not. appl.	ICESat ICE-5G
		ICE-5G*	ANU*		
		$\dot{m}$	$\dot{m}$	$\dot{m}$	$\dot{m}$
A	208	-11 ± 5	-10 ± 5	-19 ± 5	-16 ± 1
B	439	-7 ± 5	-5 ± 5	-13 ± 5	-16 ± 3
C	217	-42 ± 6	-40 ± 6	-36 ± 8	-40 ± 18
D	135	-46 ± 7	-45 ± 7	-72 ± 17	-43 ± 11
E	58	-26 ± 10	-25 ± 10	-22 ± 3	-26 ± 5
F	417	-47 ± 8	-47 ± 8	-69 ± 13	-51 ± 7
G	267	-57 ± 7	-58 ± 7	-30 ± 6	-53 ± 3
GrIS	1741	-238 ± 29	-230 ± 29	-260 ± 53	-245 ± 28

Time interval: October 2003–October 2009; $\dot{m}$ in Gt/yr.

estimates, and assuming a volume-mass density of ice of 910 kg/m^3, a fixed grounding line position and a constant velocity within the ice column, the ice exported by outlet glaciers is quantified with an accuracy of about $\pm 14\%$ (Rignot et al., 2011). The discharge data of the 38 drainage basins are aggregated into seven drainage basins optimized for the GRACE analysis by interpolating discharge values by area, if necessary. Details on the extrapolation of D to unmeasured in regions is provided in Appendix A to this letter. The annually resolved discharge for each basin is then re-sampled at monthly time intervals by linear interpolation. Then, anomalies of SMB, as well as of D are calculated w.r.t. their respective 1961–1990 mean fields, and integrated in time to obtain the cumulative storage changes of the ice sheet, comparable with the GRACE observations. From the deviation of the SMB and D reference fields (1961–1990) an additional uncertainty of the trends in cumulative difference SMB–D is estimated to be below ± 8 Gt/yr for all basins, except basin B (mean D is 17 Gt/yr larger) and ± 30 Gt/yr for the entire GrIS (Appendix A4).

2.3. ICESat

Surface elevation estimates from ICESat in the period October 2003–October 2009 (Zwally et al., 2010) are analysed to derive the mean rate of volume change of the GrIS. Data culling based on the shape of the return signal, and various quality indicators and warnings are applied to remove less reliable surface elevation estimates. The rate of elevation change, dH/dt, is derived at a resolution of 500 m along-track, by applying a least squares linear regression on all data in each 500 m segment, with the assumption that the surface elevation varies linearly with position, time and a cosine and sine terms. The total volume change is found by fitting a smooth surface, which covers the entire GrIS, through the dH/dt estimates and using the variances from the least squares regression as weights (Sørensen et al., 2011). The error on the volume change is estimated using a bootstrap approach. The observed geometric rates are corrected for elevation changes not related to ice mass changes, including firn compaction, vertical bedrock movement, and an ICESat intercampaign elevation bias. The corrected volume rate is converted into a mass balance estimate by snow/ice density modelling (Sørensen et al., 2011). The firn compaction and density models are forced by climate parameters from a high resolution regional climate model (HIRHAM5 RCM; Christensen et al., 2006) that is independent from RACMO2/GR. The uncertainty of the total mass balance is estimated to be ± 28 Gt/yr (Appendix A4).

3. Results and discussion

3.1. GrIS mass balances from GRACE, SMB–D and ICESat

For the entire GrIS, our GRACE analysis results in a mass balance of -238 ± 29 Gt/yr for October 2003–October 2009, the period with ICESat data available (Fig. 1 and Table 1). This value is consistent with our SMB–D estimates of -260 ± 53 Gt/yr, and our ICESat estimates of -245 ± 28 Gt/yr, as well as with another recent GRACE estimate of -230 ± 33 Gt/yr obtained with a different GRACE inversion strategy (from April 2002 to February 2009; Velicogna, 2009). Our estimate confirms the continental-scale comparison between GRACE and SMB–D of van den Broeke et al. (2009) and Rignot et al. (2011), and agrees within the error bars with the ensemble estimate of Schrama and Wouters (2011) based on different GRACE releases (-201 ± 19 Gt/yr; from March 2003 to February 2010), and Chen et al. (2011) (-219 ± 38 Gt/yr; from April 2002 to November 2009). For the full GRACE time series from August 2002 to September 2011, we estimate a stronger GrIS mass loss of -240 ± 18 Gt/yr, which is explained by significant acceleration of mass loss, discussed later.

Earlier GRACE estimates are to some extent discordant with our inferred rate of GrIS mass loss; e.g. Barletta et al. (2008) present a preferred ice mass loss of -101 ± 22 Gt/yr (from 2003 to early 2006), which is in good agreement with analyses from Velicogna and Wahr (2005) (from April 2002 to July 2004), Ramillien et al. (2006) and Luthcke et al. (2006), but by a factor of about two lower than the estimates of Velicogna and Wahr (2006) (from April 2002 to April 2006) and Chen et al. (2006) (from April 2002 to November 2005). Part of this discrepancy may be related to the observation period, owing to the strong interannual mass variability of the GrIS. However, truncating our time series from January 2003 to July 2005, results in GrIS mass loss of -171 ± 31 Gt/yr, which still does not lead to an agreement with Barletta et al. (2008) or Luthcke et al. (2006), despite similar observation periods. An updated mascon estimate shows a stronger mass loss of -180 ± 6 Gt/yr (August 2003–2009; Pritchard et al., 2010), yet it remains considerably below our GRACE/SMB–D/ICESat estimate for roughly the same period. The earlier ICESat estimate of -181 ± 4 Gt/yr (October

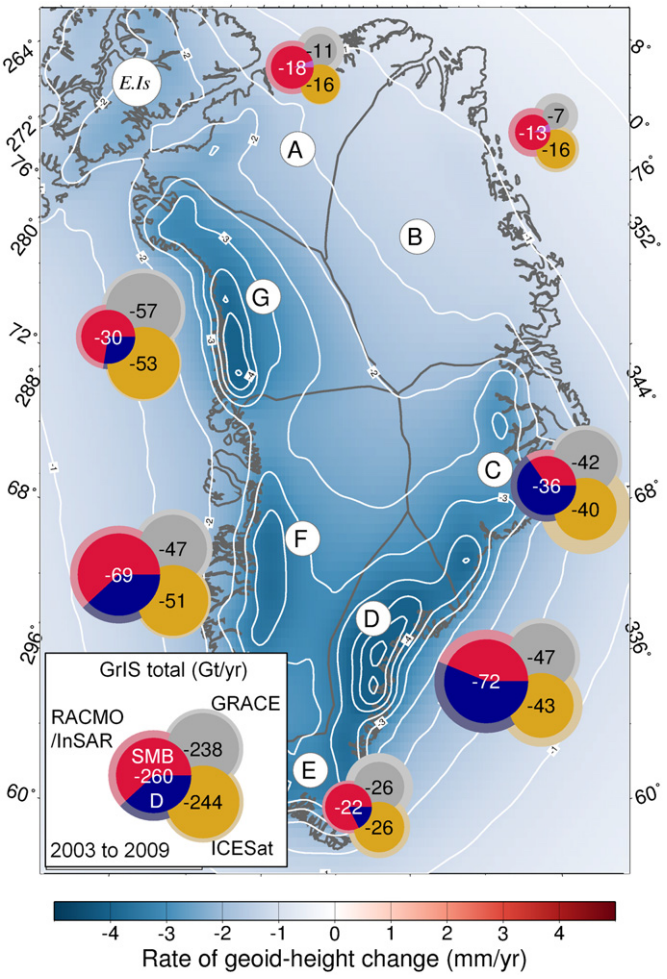

Fig. 1. Regional mass trends of the GrIS, and within seven major drainage basins (A–G) for the period October 2003–October 2009 (Gt/yr). Shown are GRACE analysis (grey circles), as well as the relative contribution of cumulative SMB anomalies (red), as well as positive (blue) and negative (magenta; -1 to -2 Gt/yr for regions A and B) cumulative D anomalies, and the trends derived from ICESat (yellow circles). Light colouring indicates uncertainties provided in Table 1. Underlain is the spatial rate of geoid-height change over Greenland calculated from the forward model adjusted to the GRACE observations. An elastic-compressible earth model is assumed and the lower and upper spherical-harmonic cut-off degrees are 2 and 340, respectively. (For interpretation of the references to colour in this figure caption, the reader is referred to the web version of this article.)

2003–2007) from Zwally and Giovinetto (2011), is broadly consistent, yet somewhat lower than our GRACE estimate for the same period (-218 ± 28 Gt/yr). Compared at the regional scale, our GRACE analysis (2003–2007) yields stronger mass loss in the west and north of the GrIS with regard to ICESat (Zwally and Giovinetto, 2011); but except for these two regions, deviations between both data sets are <10 Gt/yr.

Although a dedicated inter-comparison of GRACE analyses is yet to be undertaken, Schrama and Wouters (2011) suggest that differences can be related to treating the leakage of the gravity field signal from and to regions outside Greenland, as well as to compensating for signal attenuation due to filtering. Improved strategies for the gravity field determination of the GRACE processing centres are also relevant; the baseline accuracy of the GRACE gravity fields improved by a factor of four from RL03 to RL04. Earlier GRACE estimates based on the gravity field inversion with optimal basin averaging functions may invoke uncertainties associated with the attenuation by filtering and leakage compensating factor at least $\pm 16\%$ (Schrama and Wouters, 2011). Here, however, no calibration factor is applied, and the error on the trends associated with the filtering and inversion procedure is estimated to be $<5\%$ for the entire GrIS (Appendix A3).

3.2. Regional ice-mass balances from GRACE, SMB–D and ICESat

At the basin scale, we find agreement of GRACE, SMB–D and ICESat within their respective ranges of uncertainties (Fig. 1), for the common time interval October 2003–October 2009. In the east (C), southeast (D), southwest (F) and northwest (G) of the GrIS, GRACE and ICESat consistently exhibit mass loss stronger than ~ -40 Gt/yr, while mass loss in the northern basins A and B are much weaker (~ -15 Gt/yr). In the northwest (G), SMB–D results in smaller mass loss compared to GRACE and ICESat, which is most likely due to an underestimated D anomaly, to be addressed later. For all regions, except the east (C) and southeast (D), anomalous SMB markedly exceeds anomalous D (w.r.t. 1961–1990 mean). In the north (A) and northeast (B), the anomaly in D (w.r.t. 1961–1990 mean) is close to zero (~ -1 Gt/yr) and the mass loss is entirely explained by a distinctly lower SMB compared to the 1961–1990 mean caused by enhanced meltwater production.

3.3. Acceleration of regional ice-mass change observed by GRACE and SMB–D

The GRACE time series for the entire GrIS exhibits a statistically significant mass loss acceleration of -15 ± 7 Gt/yr^2, which is in good agreement with that of SMB–D (-21 ± 7 Gt/yr^2; common time interval August 2002–August 2010). Our estimate confirms another recent GRACE estimate of -17 ± 8 Gt/yr^2 (from April 2002 to June 2010; Rignot et al., 2011) derived with a different gravimetric inversion approach, even though, due to the large interannual mass variability of the GrIS, the exact coverage of the short time interval (9 yr for GRACE), may influence the acceleration estimates. Extending our GRACE time series until September 2011, we obtain a mass loss acceleration of -18 ± 7 Gt/yr^2, which is in good agreement with the long-term SMB–D estimate of -22 ± 1 Gt/yr^2 for the years 1992–2009 (Rignot et al., 2011). Our regional analysis locates the origin of increasingly strong mass loss primarily in the west (basin F, -16 ± 6 Gt/yr^2) and northwest (basin G, -10 ± 4 Gt/yr^2), for 2002–2011. Comparison with the accelerations from SMB–D (Table 2) reveals that on one hand, a SMB anomaly – positive from 2002 until 2005 and negative afterwards (w.r.t. 1960–1961 mean), constitutes a large part (-24 ± 3 Gt/yr^2; 2002–2010) of the apparent acceleration of for basins F and G observed with GRACE. But also increasing D by glacier speed-up accelerated mass loss by another 2 ± 1 Gt/yr^2 for basin F following a long-term trend starting in the late 1990s, and 3 ± 1 Gt/yr^2 for basin G (Fig. A2 of Appendix).

3.4. Separation of GRACE-observed mass loss into P, M/R and D

In addition to the trend and acceleration terms, Fig. 2 reveals a very high level of agreement between the time series of regional-scale GrIS mass change from GRACE and SMB–D for the common time interval August 2002–August 2010 (Fig. 2). The de-trended monthly time series (i.e. seasonal harmonic and linear trend removed) exhibit zero-lag correlations of >0.6, except for basin A (0.5) and E (0.3), which are statistically significant at the 95% confidence level, allowing us to identify the relative importance of P, M/R and D in the regional ice-mass budget. Pronounced steps in the GRACE mass loss observed in the west (basin F) are clearly related to episodes of enhanced M/R in 2002 and 2003, and from 2006 to 2008 (Fig. 2)—this is consistent with elevated seasonal maximum daily temperature anomalies (June–August) at Aassiaat, West Greenland (68.7°N, -52.8°) (Mote, 2007) in 2003, 2005 and 2007, as well as record melt extent for the entire GrIS in these years (Fettweis et al., 2011).

3.5. Changes in the northwest of the GrIS

In the northwest (basin G), this and other GRACE analysis (Khan et al., 2010; Schrama and Wouters, 2011; Chen et al., 2011) indicate a rapid transition to stronger negative mass balances after summer 2005, an area which has been dynamically thinning since the 1990s (Krabill et al., 2000). Regarding the main SMB constituents our analysis indicates that P is important in explaining the abrupt change in trend as a consequence of higher accumulation (i.e. higher SMB) before the year 2005, and lower afterwards w.r.t. the 1961–1990 mean (Fig. 2). Starting in winter 2009/2010, enhanced accumulation again slightly weakens the negative ice-mass balance observed with GRACE; the mass loss in the west (basin F), however, remains strongly negative for the year 2011.

It should be noted, however, that the agreement between SMB–D and GRACE is somewhat poorer in the northwest (basin G) than in other basins. We consider the GRACE trend to be more reliable due to the agreement with our ICESat estimate in the period 2003–2009 (Fig. 1). In addition, the distinct shift in the GRACE time series to stronger negative mass balances is recorded with the GPS station Thule (76.5°N, -68.8°) showing a similar temporal behaviour in the deformation of the elastic lithosphere, induced by changes in the ice mass balance (Khan et al., 2010). Moreover, localized surface-lowering in this area detected with ICESat (Fig. A3 of Appendix) between 2003 and 2008 is also an indication of considerable glacier thinning. This may have been missed in the estimates of D due to incomplete ice thickness mapping in this region (Rignot and Kanagaratnam, 2006). Considering that glacier speed-up and ice-front retreat between 2000/2001 and 2005/2006 have been documented for the northwest (Joughin et al., 2010), in addition to P, part of the change in trend observed with GRACE could be related to, potentially rapid, changes in D. If we consider GRACE minus SMB–D as an estimate for the missing portion of D, we deduce that non-surveyed dynamic thinning could be responsible for an additional 24 ± 13 Gt/yr of mass loss, implying an imbalance for the entire region of about 40% (w.r.t. 1961–1990).

3.6. Changes in the southeast of the GrIS

In other regions, our comparison of GRACE and the SMB components shows that P dominates the temporal mass variations observed with GRACE during 8-yr time period (2002–2010). For example, in the high-accumulation regions in the east of the GrIS

Table 2
Regional mass trends and accelerations of the GrIS from GRACE and SMB–D for the common time interval August 2002–August 2010, as well as the trends and acceleration for the individual components of SMB–D; cumulative anomalies (w.r.t. 1961–1990 mean) in total precipitation (P), melting/run-off (M/R) and discharge (D). The GRACE results are provided for CSR RL04 and the GIA correction ICE-5G* (Appendix A3).

Drainage basin	Area (10^3 km^2)	GRACE CSR RL04		RACMO2/GR+InSAR							
		(ICE-5G*)		SMB–D		P		M/R		D	
		$\dot{m}$	$\ddot{m}$	$\dot{m}$	$\ddot{m}$	$\dot{m}$	$\ddot{m}$	$\dot{m}$	$\ddot{m}$	$\dot{m}$	$\ddot{m}$
A	208	-16 ± 5	-3 ± 3	-20	-2	-2	-1	19	n.sig.	-1	n.sig.
B	439	-12 ± 6	4 ± 4	-16	n.sig.	7	1	25	n.sig.	-3	n.sig.
C	217	-39 ± 7	8 ± 5	-31	2	3	3	13	-1	22	1
D	135	-43 ± 6	n.sig.	-66	4	-14	n.sig.	12	n.sig.	41	-5
E	58	-23 ± 6	n.sig.	-20	-3	-3	-4	14	-1	4	n.sig.
F	417	-45 ± 8	-12 ± 6	-66	-11	6	-10	45	n.sig.	26	2
G	267	-50 ± 6	-16 ± 4	-26	-13	n.sig.	-8	18	1	7	3
GrIS	1741	-228 ± 22	-15 ± 7	-244	-21	n.sig.	-19	145	n.sig.	96	3

Time interval: August 2002–August 2010; $\dot{m}$ in Gt/yr, $\ddot{m}$ in Gt/yr^2; n. sig., statistically not significant.

(Ettema et al., 2009), synchronous events of enhanced precipitation temporarily offset the otherwise persistent negative mass balances in the winter of 2002/2003 (basins C and D). Here, GRACE records a mass gain around 131–211 Gt (large uncertainty due to early GRACE data), or 0.3–0.4 m equivalent water height over basins C+D+E, between August 2002 and April 2003, representing twice the 2002–2010 average accumulation for these months. In the east (C), a similar accumulation event took place between August 2008 and April 2009, causing a mass gain of around 72–96 Gt ($\sim$0.3 m equivalent water height). In these years, the accumulation anomalies outweighed the losses by M/R and D that prevailed during 2003–2008, and after summer 2010. Most of the reduction mass loss rates in the southeast previously attributed to decreasing flow speeds (Chen et al., 2011) can be explained by these accumulation events. Fitting a quadratic function to the GRACE time series (2002–2011) results in an apparent net mass-loss deceleration of $+6\pm5$ Gt/yr^2 for basin C, exemplifying how regionally diverse the sources of GrIS mass variability within the last decade have been.

3.7. Changes in the north of the GrIS

The moderate negative mass balances in the north (A) and northeast (B) of the GrIS (-16 ± 5 Gt/yr and -12 ± 5 Gt/yr, respectively; GRACE for 2002–2011) are mainly caused by reduced SMB due to enhanced M/R, modulated by a 1- (A) and 2-yr (B) period of mass gain starting in winter 2005/2006. For Ellesmere Island, located $\sim$40 km northwest of the GrIS at its closest point, mass loss is -35 ± 5 Gt/yr and significantly accelerating at -8 ± 5 Gt/yr^2 (GRACE for 2002–2011), which is consistent with another recent estimate from GRACE, SMB–D and ICESat (Gardner et al., 2011). On Ellesmere Island, however, a gradual increase in M/R in direct response to increasing summer temperatures (Gardner et al., 2011) induces most of this acceleration ($+6\pm1$ Gt/yr^2; 2002–2010), indicating a sensitive response of this region to the climatic forcing.

4. Conclusion

For all regions and the GrIS as a whole, the trends imposed by anomalies in M/R and D after 9-yr (2002–2011) significantly exceed decadal variability of trends in P for 1958–2010, meaning that GRACE and ICESat record long-term changes of the GrIS. For the west and northwest (basins F and G, respectively), the joint acceleration of M/R and D, significantly exceed the interannual variability in P, suggesting that, despite a strong contribution of P, 9-yr of GRACE data contain a long-term climate signal of mass loss acceleration in these regions (-26 ± 7 Gt/yr^2; basin F+G; 2002–2011). Part of the recent apparent acceleration is, however, due to gradual variations in P. For the GrIS as a whole, interannual mass variability during the 9-yr period mainly arises from P variations in the east (basin C), southeast (basin D) and west (basin F), and obscures the acceleration of M/R and D persisting since the 1990s (Fig. A2 of Appendix). Weaker mass loss rates observed with GRACE in the east (basin C) and to a lesser extent in the southeast (basin D) after winter 2008/2009, which have previously been attributed to decreasing ice-dynamic flow (Chen et al., 2011), are mainly a consequence of enhanced accumulation.

In summary, we show that GRACE, SMB–D and ICESat data (October 2003–October 2009) are sufficiently mature to provide consistent regional scale mass balances of the GrIS. This yields new insight into the complex mass loss behaviour of the GrIS showing that all mass balance components (P, M/R and D) are relevant in the regional mass budget. In particular, we demonstrate that variations in P substantially influence the year-to-year ice-mass balance, and care has to be taken in interpreting GRACE-derived net mass changes in terms of changing ice dynamics. We find that currently (2002–2010) that the M/R production is enhanced by at least 39–59% compared to 1961–1990 for all basins, but most significantly in the northwest (basin G; 90–134%), whereas D is up to 40–60% larger in the east (basin C). For all basins, M/R has more strongly increased than D for the entire GrIS (50–74% for M/R and 18–27% for D, w.r.t. 1961–1990), owing to the sensitivity of M/R compared to D to increasing surface-air temperature, observed in the Arctic during last decade (Hanna et al., 2008). It remains to be seen, whether dynamic thinning will follow this melting trend, particularly in the north (basin A), where M/R increased by 75–111% (compared to 1961–1990 mean), and so far only minor changes in ice flow are observed (Moon and Joughin, 2008). Continuous satellite and *in situ* observations will be important to place increasing confidence on the long-term trends and follow the ongoing evolution of the GrIS.

Acknowledgments

Ingo Sasgen would like to acknowledge support from the Deutsche Forschungsgemeinschaft (DFG, German Research Foundation) through Grant SA 1734/2-2 (SPP1257). We would like to thank the German Space Operations Center (GSOC) of the German Aerospace Center (DLR) for providing continuously and nearly 100% of the raw telemetry data of the twin GRACE satellites. This

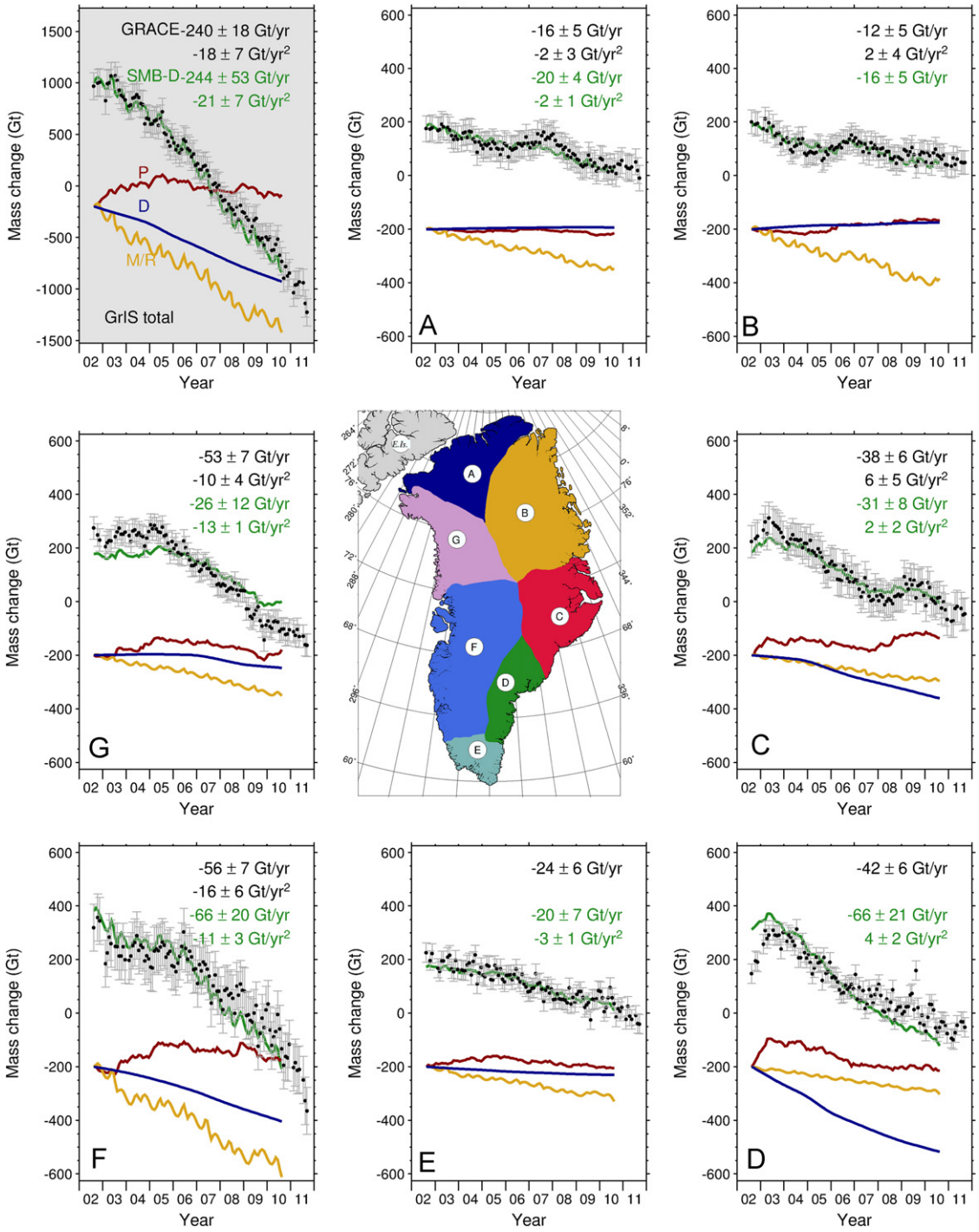

Fig. 2. Regional mass variation of the GrIS, and within seven major drainage basins (A–G) from GRACE (black circles and black values; August 2002–August 2011) and cumulative anomalies in SMB–D (green curves and green values; August 2002–August 2010). SMB–D is further divided into its main constituents, cumulative anomalies of precipitation (P; red), melting/run-off (R; orange) and discharge (D; blue)—for easier comparison with GRACE, both M/R and D are plotted with opposite sign. If statistically significant, trend and acceleration terms are indicated for the GRACE and SMB–D for the respective time interval. Details on the GIA correction are provided in the Appendix A. (For interpretation of the references to colour in this figure legend, the reader is referred to the web version of this article.)

work is a contribution to the "Helmholtz Climate Initiative REKLIM" (Regional Climate Change), a joint research project of the Helmholtz Association of German research centres (HGF). Michiel van den Broeke acknowledges support from Utrecht University, the RAPID international project and the Netherlands Polar Programme. This work was supported by funding from the ice2sea programme from the European Union 7th Framework Programme, Grant no. 226375. Ice2sea contribution number ice2sea039. We would like to thank Philippe Lucas-Picher for the high resolution HIRHAM5 data. We would like to thank four anonymous reviewers for their helpful comments.

Author contribution: Ingo Sasgen developed the study, carried out the GRACE analysis and performed the GIA modelling; Bert Wouters and Isabella Velicogna assisted with the GRACE analysis; Michiel van den Broeke provided the SMB time series; D was provided by Eric Rignot; Jonathan L. Bamber assisted with the SMB–D analysis; Louise Sandberg Sørensen analysed the ICESata data; Zdeněk Martinec assisted with the development of the GRACE

methodology and provided his GIA modelling code; Sebastian B. Simonsen converted ICESat volume changes to mass changes by firn compaction and density modelling; all authors discussed the material presented and contributed to the writing of the manuscript.

Appendix A. Supplement to data sets and methods

A.1. GRACE post-processing

In this study, 103 unconstrained monthly mean GRACE gravity field solutions of the Centre for Space Research University of Texas, Austin, USA (CSR RL04; August 2002 to September 2011 Bettadpur, 2007) are filtered and inverted for mass changes using a forward modeling approach (Sasgen et al., 2010). This involves calculating the gravity field signal for each drainage basin and Ellesmere Island for a predefined mass change distribution — here, is based on the standard deviation of the mass variability of RACMO2/GR for the years January 2002 to December 2008 (74 months), assuming an elastic-compressible earth (Farrell, 1972; Wahr et al., 1998). Our forward model localizes the mass changes more in the coastal areas of GrIS and for Ellesmere Island in the ice covered areas compared to a uniform mass distribution, which leads to a less biased inverse solution. Changes in D are not prescribed in the forward model, and the uncertainty caused by this simplification is assessed by inverting the GRACE gravity fields with an alternative forward model based on ICESat data, which reflects both, changes in SMB and D. The errors associated with our inversion method are detailed in Appendix A.2.

The prescribed mass distribution for all drainage basins is simultaneously adjusted in magnitude such that the misfit between the predicted and GRACE-observed spatial gravity field changes, both identically filtered, is minimized in a least-squares sense. The seven drainage basins (henceforth, drainage basins A to G, Fig. 1) are defined according to the principal ice divides inferred from balance ice-velocities (Hardy et al., 2000). For Ellesmere Island, we adopt all areas that are ice covered in RACMO2/GR. The number of GrIS basins and their spatial separation is chosen to allow for recovering nearly independent estimates of mass change (Schrama and Wouters, 2011). The monthly GRACE coefficients are smoothed with an isotropic (i.e. degree-dependent) spatial averaging function (Sasgen et al., 2006), which optimizes the trade-off between spatial resolution – typically between 400 and 500 km – and noise with respect to the expected signals. The monthly coefficients of degree 2 and order 0 from GRACE are not reliable and are substituted by an estimate from Satellite Laser Ranging (Cheng and Tapley, 2004). For further regionalization, the weight of low degree and order coefficients are reduced according to the correlation of the predicted GrIS mass signal and its superposition with GIA in response to the history Laurentide ice sheet (Fig. A.1). Our inversion scheme for the GRACE solutions is validated with a simulated time series of monthly gravity-field variations based on cumulative RACMO2/GR mass anomalies for the years 2002 to 2008, w.r.t 1961 to 1990.

To derive the long-term trends, the annual-oscillating component is removed from the monthly time series of GRACE mass anomalies, then, the time series are expanded into the first three Legendre polynomials. The advantage of a fit with Legendre polynomials is that the resulting trend and acceleration time series are orthogonal, providing independent estimates that are insensitive to a small change in the observation interval. The statistic significance of each term is determined using a Student *t*-test, estimating errors from the regression residuals and assuming a confidence limit of 5%.

A.2. GRACE error budget

Formal, as well as calibrated errors provided with the GRACE solutions of Stokes potential coefficients underestimate the true uncertainties, as they do not account for uncertainties associated with the de-aliasing models of atmospheric and oceanic short-term variability. Therefore, we derive an empirical error estimate from the difference between two largely independent sets of GRACE coefficients, the CSR RL04 (Bettadpur, 2007) and GFZ RL04 (Flechtner, 2007). Although both GRACE releases rely on similar processing standards and background models, differences in the details of the gravity field determination cause deviations of the

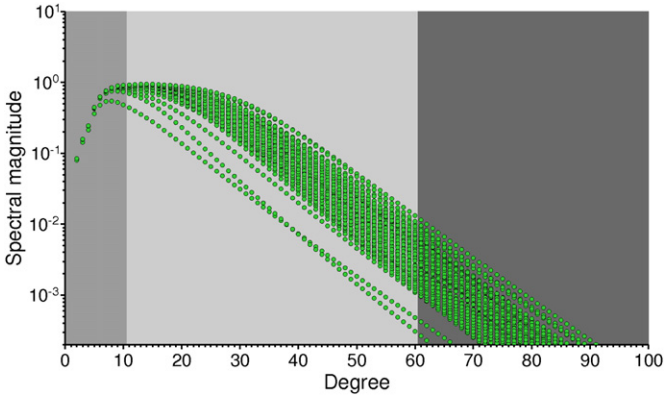

Fig. A.1. Filter response function applied to the monthly GRACE gravity field coefficients. Damping in the lower spectral part (medium shaded) accounts for the degree-correlation between the predicted GrIS mass change signal and its superpositions with the Laurentide GIA signal, whereas damping in the medium spectral part (light shaded) follows the signal-to-noise ratio in the GRACE coefficients. The upper limit of cut-off degree and order 60 (dark shaded) is governed by availability of the GRACE coefficients in CSR RL04.

Table A1
Uncertainties of GRACE-inferred mass change for monthly solutions and linear trends for the seven major drainage basins (Fig. 1). Total uncertainties (Total) constitute the empirical errors in the GRACE gravity field solutions estimated from the difference between CSR RL04 and GFZ RL04 (Rel.), the filtering and inversion procedure (Filt./Inv.), the *a priori* assumption on the mass distribution (Forw. Model), and, in the case of the linear trend and acceleration terms, of formal regression errors (Regr.). Also provided is the range of plausible GIA corrections (GIA).

Drainage basin	Area (10^3 km^2)	Monthly GRACE uncert. (Gt)				Lin. trend GRACE uncert. (Gt/yr)					Acceleration GRACE uncert. (Gt/yr^2)					GIA range (Gt/yr)	
		Rel.	Filt./Inv.	Forw. model	Total	Rel.	Filt./Inv.	Forw. model	Regr.	Total	Rel.	Filt./Inv.	Forw. Model	Regr.	Total	+min	+max
A	208	45	3	14	47	1	<1	4	2	5	2	1	1	2	3	−1	6
B	439	43	9	9	45	1	3	2	2	5	1	1	1	2	4	<1	5
C	217	58	12	9	60	1	4	2	3	6	<1	2	2	2	5	−1	4
D	135	84	11	21	87	6	1	1	3	7	<1	1	4	3	5	−1	3
E	58	65	9	12	67	4	1	2	3	5	1	1	<1	2	3	−1	1
F	417	84	13	21	88	4	<1	4	4	7	<1	4	2	3	6	−2	7
G	267	38	16	9	42	3	4	3	2	7	2	2	<1	2	4	−5	2
GrIS	1741	131	16	21	134	15	8	8	6	18	2	2	5	5	7	−3	20

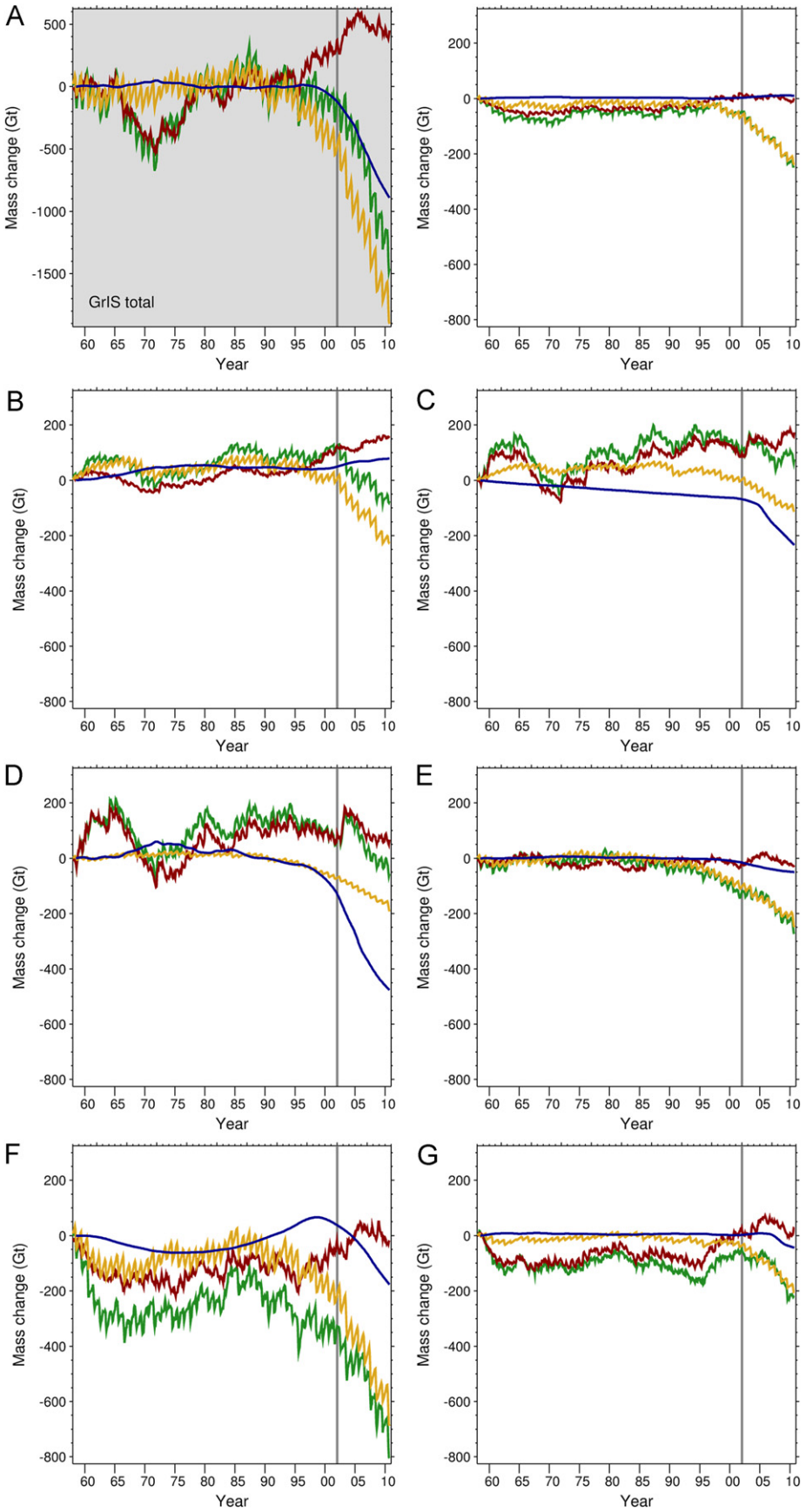

Fig. A.2. Cumulative mass anomaly of P (red), R (yellow), SMB (green) and D (blue) between 1958 and 2010 for GrIS (w.r.t. 1961–1990 mean), for the seven major drainage basins (Fig. 1). The starting date for the availability of GRACE monthly solutions (April 2002) is indicated by the vertical grey line.

gravity field solution, and the inferred mass-change estimate (Table A.1). In addition, we estimate the uncertainty associated with our filtering and inversion scheme by performing our calculation on simulated (error-free) GRACE solutions. We also test the sensitivity of our estimates on the predefined mass change distribution (here, based on RACMO2/GR), by inverting the actual GRACE solutions with an alternative forward model based on mass trends inferred from ICE-Sat elevation changes (Fig. A.3). The uncertainty introduced by GIA is discussed in the following section. It should be stated that the applied inversion scheme and its accuracy stated in Table A.1 reflects our current understanding of GRACE processing, although alternative methods using e.g. Mascon (Luthcke et al., 2008) or optimal basin averaging functions (Velicogna, 2009) may perform similarly well.

A.3. Correcting for glacial-isostatic adjustment

In the GRACE trends over Greenland, GIA signature require removal, that are associated with the history of GrIS itself, as well as with the recession of the Laurentide ice sheet in North America, following the last glacial maximum. For the Laurentide GIA signal the GRACE trends can serve as a new constraint (e.g Tamisiea et al., 2007), augmenting more traditional measurements like GPS and tide-gauges (Davis and Mitrovica, 1996; Braun et al., 2008), terrestrial gravity, satellite radar altimetry (Lee et al., 2008), traditional leveling or sea-level indicators (e.g. Tushingham and Peltier, 1992; Lambeck et al., 1998).

To minimize the influence of GIA on the GrIS mass trends from GRACE, and to assess their uncertainty on the GrIS mass change derived from GRACE, we proceed as follows. First, GIA induced by the GrIS and Laurentide ice sheet are modeled independently; for the GrIS the glacial reconstruction of Fleming and Lambeck (2004) is adopted, for North America, the Lauren-tide ice sheet component of ICE-5G is isolated. Following the approach of Paulson et al. (2007), the total glacial load of the Laurentide ice sheet component of ICE-5G is adjusted in order to minimize the misfit between the predicted and GRACE-inferred trends in gravity fields over the Hudson Bay, North America (adjusted version is denoted as ICE-5G*). In advance to the adjustment, the GIA prediction is filtered identically to the GRACE trends, and the GRACE trends are corrected for variations in total water storage estimated with the hydrology model WGHM (Döll et al., 2003). It should be mentioned, that the adjustment of GIA over North America is optimal only with respect to the band-pass filtered GRACE coefficients.

To estimate the uncertainty of our GIA correction, the scaling procedure is repeated for a variety of viscosity models ranging between 2×10^{20} Pa s and 8×10^{20} Pa s for the upper mantle and 5×10^{21} Pa s and 4×10^{22} Pa s for the lower mantle, for thickness of the lithosphere of 80, 100 and 120 km, as well as for the glacial history ANU (Lambeck and Chappell, 2001) developed at the Australian National University (adjusted version is denoted as ANU*). In terms of the GIA related to the glacial history of the GrIS, GRACE provides no useful additional constraint, because the GIA signal directly underlays that of ongoing ice-mass changes. We estimate the related uncertainty by varying upper- and lower-mantle viscosities in the range stated above. For ICE-5G* and the glacial history of GrIS, upper- and lower mantle viscosities of 6×10^{20} Pa s and 2×10^{22} Pa s are adopted as reference values; for the Laurentide component of ANU* we employ 5×10^{20} Pa s and 1×10^{22}.

A.4. Regional climate modelling and InSAR satellite observations

The attribution of GRACE-inferred mass losses to anomalies in SMB or D requires the definition of a reference period during which the Greenland ice sheet was approximately in balance, i.e. SMB $\approx$ D. The 30-year time interval from 1961 to 1990 may serve as such a period, as it provides a meaningful multi-decadal climatology that excludes large SMB variations and imbalance starting in the year 1996. Therefore, for all basins, the anomalies in SMB and D are calculated separately with respect to the means for the years 1961–1990. The deviation of the SMB and D mean fields (1961–1990) provides an indication of the systematic uncertainties in the SMB and D data sets, and the approach of combining their anomalies in SMB-D; the difference of mean D and mean SMB is <8 Gt/yr for all basins, except basin B (mean D is 17 Gt/yr larger), for the GrIS the uncertainty is estimated to $\pm$ 14%. In the case of D, estimates are not continuous prior to 1996 (Rignot et al., 2008; Rignot and Kanagaratnam, 2006). To interpolate D between years with observations we correlated D with averaged runoff for the preceding four years and current year. This is similar to a previous approach (Rignot et al., 2008) except here we use runoff rather than SMB and we use estimates from RACMO2/GR. For the ice covered area in RACMO2/GR, that is unsurveyed by ($\sim$12%; Rignot and Kanagaratnam, 2006), the D anomalies are assumed to be 0. In addition, D data are extrapolated to areas of basin F and basin G, which were problematic to survey with InSAR (basin 38; Rignot and Kanagaratnam, 2006), as follows: first, the mean D (years 1961–1990) is scaled by the factor "total area"/"surveyed area", resulting in 1.1 for basin F and 1.5 for basin G. Here, "total area" refers to the spatial coverage of the InSAR survey provided in (Rignot and Kanagaratnam, 2006), covering 99% (F) and and 92% (G) of the ice covered area in RACMO2/GR. Then, a regional "imbalance" factor for each year between 2002 and 2008 is applied to the mean D of the unsurveyed area; for basin G, the imbalance factor for drainage basin number 25 in the InSAR data set of Rignot and Kanagaratnam (2006) is adopted, whereas for basin F the factor is based on the average of the neighbouring basins number 21, 22 and 23 (Rignot and Kanagaratnam, 2006). Then, the extrapolated D minus the mean D for 1961–1990 of the unsurveyed region is calculated, and added to the surveyed D anomalies. For all basins, due to the unavailability of data, D is assumed to remain unchanged in 2010, compared to 2009. The time series of the SMB components and D evaluated for each basin from 1958 to 2010 are shown in Fig. A.2. For Ellesmere Island, D anomalies are assumed to be zero due to lack of recent data. Since the 1999–2003 mean D is estimated to be 5 ± 2 Gt/yr (Gardner et al., 2011, Suppl. Information), the error introduced by our assumptions is small compared to the GRACE-estimated trend.

A.5. ICESat observations

NASA's ICESat carried the Geoscience Laser Altimeter System (GLAS) instrument (Zwally et al., 2010), which performed ice sheet elevation measurements in the period 2002–2009. Here, ICESat altimetry measurements from the GrIS and the surrounding glaciers and ice caps are considered in the elevation change analysis. The rejection of problematic measurements reduced the number of measurements by approximately 13%. The total volume change of the GrIS from October 2003 to October 2009 is found by fitting a smooth surface covering the entire ice sheet, through the ICESat derived rate of surface-elevation change. This geometric rate of ice sheet loss is related to mass, by correcting for volume losses not contributing to a mass loss and applying the appropriate conversion density to the corrected volume (Sørensen et al., 2011). The correction terms are firn compaction, vertical bedrock movement, and ICESat intercampaign elevation bias. The derived rate of elevation changes, corrected for these terms are shown in Fig. A.3. The firn compaction term is by far the largest of the corrections applied. Both the surface density model, and the firn compaction model are forced by surface temperature,

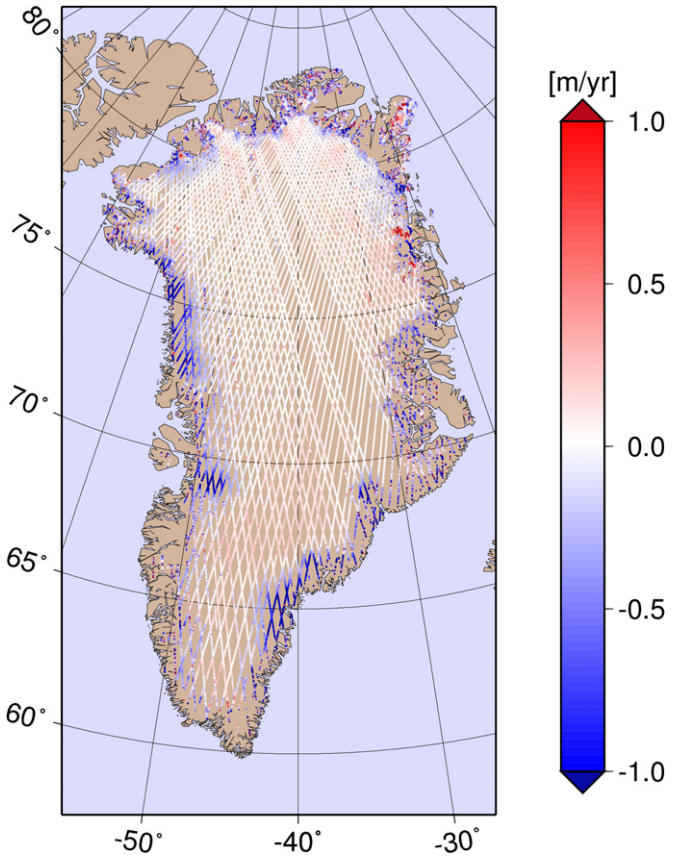

Fig. A.3. Rate of elevation changes derived from ICESat measurements, and corrected for elevation changes caused by firn compaction, vertical bedrock movement and ICESat intercampaign bias.

accumulation and run-off from a high resolution regional climate model (HIRHAM5 RCM). The HIRHAM5 RCM simulation covering the period from 1989 to 2009, and are driven by the ERA-Interim re-analysis product, at the lateral boundaries.

An independent error analysis has been conducted for each of the drainage basins to estimate the regional error associated with the derived mass balance of the GrIS. This error analysis consists of six error sources, which are assumed to be independent; ICESat volume estimates, ICESat intercampaign bias, vertical bedrock movement, firn compaction, neglecting basal melt and using simplified assumptions on ice dynamics (Sørensen et al., 2011). A bootstrap procedure has been applied to estimate the regional error from the sampling and interpolation of the measured surface elevation change in the ICESat tracks. Both the firn compaction modelling and the vertical bedrock correction are associated with a volume error estimate. The error on the corresponding mass change has been estimated by regionally adding a perturbation of the volume error and applying the density model. By neglecting basal melt and using simplified assumptions on ice dynamics—possible build up of ice above the equilibrium line altitude (ELA), an error may be present in areas above the ELA, which are associated with an elevation increase. This error contribution is determined by the difference between the applied density of firn and the density of ice, and the magnitude of the ice dynamics are determined by a simple flow model (Sørensen et al., 2011).

References

Ablain, M., Cazenave, A., Valladeau, G., Guinehut, S., 2009. A new assessment of the error budget of global mean sea level rate estimated by satellite altimetry over 1993–2008. Ocean Sci. 5, 193–201.

Barletta, V.R., Sabadini, R., Bordoni, A., 2008. Isolating the PGR signal in the GRACE data: impact on mass balance estimates in Antarctica and Greenland. Geophys. J. Int. 172 (1), 18–30.

Bartholomew, I., Nienow, P., Mair, D., Hubbard, A., King, M.A., Sole, A., 2010. Seasonal evolution of subglacial drainage and acceleration in a Greenland outlet glacier. Nat. Geosci. 3 (6), 408–411.

Bettadpur, S., 2007. CSR Level-2 Processing Standards Document for Level-2 Product Release 04, Rev. 3.1, GRACE 327-742 (CSR-GR-03-03). University of Texas, Austin.

Box, J.E., Bromwich, D.H., Bai, L.-S., 2004. Greenland ice sheet surface mass balance 1991–2000: application of Polar MM5 mesoscale model and in situ data. J. Geophys. Res. 109 (D16105).

Box, J.E., Cappelen, J., Decker, D., Fettweis, X., Mote, T., Tedesco, M., van de Wal, R.S.W., 2010. Greenland. In: Richter-Menge, J., Overland, J.E. (Eds.), Arctic Report Card 2010. National Oceanic and Atmospheric Administration, Washington, DC, pp. 55–64.

Braun, A., Kuo, C.-Y., Shum, C.K., Wu, P., van der Wal, W., Fotopoulos, G., 2008. Glacial isostatic adjustment at the Laurentide ice sheet margin: models and observations in the Great Lakes region. J. Geodyn. 46 (3–5), 165–173.

Cazenave, A., 2006. How fast are the ice sheets melting? Science 314 (5803), 1250–1252.

Chen, J.L., Wilson, C.R., Tapley, B.D., 2006. Satellite gravity measurements confirm accelerated melting of Greenland ice sheet. Science 313, 1958–1960.

Chen, J.L., Wilson, C.R., Tapley, B.D., 2011. Interannual variability of Greenland ice losses from satellite gravimetry. J. Geophys. Res. 116, B07406.

Cheng, M., Tapley, B., 2004. Variations in the Earth's oblateness during the past 28 years. J. Geophys. Res. 109, B0940.

Christensen, O.B., Drews, M., Christensen, J., Dethloff, K., Ketelsen, K., Hebestadt, I., Rinke, A., 2006. The HIRHAM Regional Climate Model. In: Danish Meteorological Institute Technical Report Series. Cambridge University Press.

Davis, J.L., Mitrovica, J.X., 1996. Glacial isostatic adjustment and the anomalous tide gauge record of eastern North America. Nature 379 (6563), 331–333.

Döll, P., Kaspar, F., Lehner, B., 2003. A global hydrological model for deriving water availability indicators: model tuning and validation. J. Hydrol. 270 (1–2), 105–134.

Ettema, J., van den Broeke, M.R., van Meijgaard, E., van de Berg, W.J., Bamber, J.L., Box, J.E., Bales, R.C., 2009. Higher surface mass balance of the Greenland ice sheet revealed by high-resolution climate modeling. Geophys. Res. Lett. 36 (12), L12501.

Farrell, W.E., 1972. Deformation of the earth by surface loads. Rev. Geophys. 10, 761–797.

Fettweis, X., Tedesco, M., van den Broeke, M., Ettema, J., 2011. Melting trends over the Greenland ice sheet (1958–2009) from spaceborne microwave data and regional climate models. Cryosphere 5 (2), 359–375.

Flechtner, F., 2007. GFZ Level-2 Processing Standards Document for Level-2 Product Release 04, Rev. 1.0, GRACE 327-743 (GR-GFZ-STD-001). GeoForschungsZentrum Potsdam.

Fleming, K., Lambeck, K., 2004. Constraints on the Greenland ice sheet since the last glacial maximum from sea-level observations and glacial-rebound models. Q. Sci. Rev. 23, 1053–1077.

Gardner, A.S., Moholdt, G., Wouters, B., Wolken, G.J., Burgess, D.O., Sharp, M.J., Cogley, J.G., Braun, C., Labine, C., 2011. Sharply increased mass loss from glaciers and ice caps in the Canadian Arctic Archipelago. Nature 473 (7347), 357–360.

Hanna, E., Huybrechts, P., Cappelen, J., Steffen, K., Bales, R.C., Burgess, E., McConnell, J.R., Steffensen, J.P., Van den Broeke, M., Wake, L., Bigg, G., Griffiths, M., Savas, D., 2011. Greenland ice sheet surface mass balance 1870 to 2010 based on twentieth century reanalysis, and links with global climate forcing. J. Geophys. Res. 116, D24121.

Hanna, E., Huybrechts, P., Janssens, I., Cappelen, J., Steffen, K., Stephens, A., 2005. Runoff and mass balance of the Greenland ice sheet: 1958–2003. J. Geophys. Res. 110, D13108.

Hanna, E., Huybrechts, P., Steffen, K., Cappelen, J., Huff, R., Shuman, C., Irvine-Fynn, T., Wise, S., Griffiths, M., 2008. Increased runoff from melt from the Greenland Ice Sheet: a response to global warming. J. Climate 21 (2), 331–341.

Hardy, R., Bamber, J., Orford S., 2000. The delineation of drainage basins on the Greenland ice sheet for mass-balance analyses using a combined modelling and geographical information system approach. Hydrol. Process. 14 (11–12), 1931–1941.

Holland, D.M., Thomas, R.H., de Young, B., Ribergaard, M.H., Lyberth, B., 2010. Acceleration of Jakobshavn Isbrae triggered by warm subsurface ocean waters. Nat. Geosci. 1 (10), 659–664.

Joughin, I., Smith, B.E., Howat, I.M., Scambos, T., Moon, T., 2010. Greenland flow variability from ice-sheet-wide velocity mapping. J. Glaciol. 56 (197), 415–430.

Khan, S.A., Wahr, J., Bevis, M., Velicogna, I., Kendrick, E., 2010. Spread of ice mass loss into northwest Greenland observed by GRACE and GPS. Geophys. Res. Lett. 37, L06501.

Krabill, W., Abdalati, W., Frederick, E., Manizade, S., Martin, C., Sonntag, J., Swift, R., Thomas, R., Wright, W., Yungel, J., 2000. Greenland ice sheet: high-elevation balance and peripheral thinning. Science 289 (5478), 428–430.

Krabill, W., Hanna, E., Huybrechts, P., Abdalati, W., Cappelen, J., Csatho, B., Frederick, E., Manizade, S., Martin, C., Sonntag, J., Swift, R., Thomas, R., Yungel, J., 2004. Greenland ice sheet: increased coastal thinning. Geophys. Res. Lett. 31, L24402.

Lambeck, K., Chappell, J., 2001. Sea-level change throughout the last-glacial cycle. Science 292 (5517), 679–686.

Lambeck, K., Smither, C., Ekman, M., 1998. Tests of glacial rebound models for Fennoscandinavia based on instrumented sea- and lake-level records. Geophys. J. Int. 135, 375–387.
Lee, H., Shum, C.K., Yi, Y., Braun, A., Kuo, C.-Y., 2008. Laurentia crustal motion observed using TOPEX/POSEIDON radar altimetry over land. J. Geodyn. 46 (3–5), 182–193.
Luthcke, S.B., Arendt, A.A., Rowlands, D.D., McCarthy, J.J., Larsen, C.F., 2008. Recent glacier mass changes in the Gulf of Alaska region from GRACE mascon solutions. J. Glaciol. 54, 767–777.
Luthcke, S.B., Zwally, H.J., Abdalati, W., Rowlands, D.D., Ray, R.D., Nerem, R.S., Lemoine, F.G., McCarthy, J.J., Chinn, D.S., 2006. Recent Greenland ice mass loss by drainage system from satellite gravity observations. Science 314, 1286–1289.
Moon, T., Joughin, I., 2008. Changes in ice front position on Greenland's outlet glaciers from 1992 to 2007. J. Geophys. Res. 113, F02022.
Mote, T.L., 2007. Greenland surface melt trends 1973–2007: evidence of a large increase in 2007. Geophys. Res. Lett. 34, L22507.
Nghiem, S.V., Rigor, I.G., Perovich, D.K., Clemente-Colón, P., Weatherly, J.W., Neumann, G., 2007. Rapid reduction of Arctic perennial sea ice. Geophys. Res. Lett. 34, L22507.
Paulson, A., Zhong, S., Wahr, J., 2007. Inference of mantle viscosity from GRACE and relative sea level data. Geophys. J. Int. 171 (2), 497–508.
Peltier, W.R., 2004. Global glacial isostasy and the surface of the ice-age earth: the ICE5G (VM2) model and GRACE. Annu. Rev. Earth Planet. Sci. 32, 111–149.
Pritchard, H.D., Luthcke, S.B., Fleming, A.H., 2010. Understanding ice-sheet mass balance: progress in satellite altimetry and gravimetry. J. Glaciol. 56.
Ramillien, G., Lombard, A., Cazenave, A., Ivins, E.R., Llubes, M., Remy, F., Biancale, R., 2006. Interannual variations of the mass balance of the Antarctica and Greenland ice sheets from GRACE. Global Planet. Change 53 (3), 198–208.
Rignot, E., Bamber, J.L., Van Den Broeke, M.R., Davis, C., Li, Y., Van De Berg, W.J., Van Meijgaard, E., 2008. Recent Antarctic ice mass loss from radar interferometry and regional climate modelling. Nat. Geosci. 1 (2), 106–110.
Rignot, E., Kanagaratnam, P., 2006. Changes in the velocity structure of the Greenland ice sheet. Science 311 (5763), 986–990.
Rignot, E., Koppes, M., Velicogna, I., 2010. Rapid submarine melting of the calving faces of West Greenland glaciers. Nat. Geosci. 3 (3), 187–191.
Rignot, E., Velicogna, I., van den Broeke, M.R., Monaghan, A., Lenaerts, J., 2011. Acceleration of the contribution of the Greenland and Antarctic ice sheets to sea level rise. Geophys. Res. Lett. 38, L05503.
Sasgen, I., Martinec, Z., Bamber, J., 2010. Combined GRACE and InSAR estimate of West Antarctic ice-mass loss. J. Geophys. Res. 115, F04010.
Sasgen, I., Martinec, Z., Fleming, K., 2006. Wiener optimal filtering of GRACE data. Stud. Geophys. Geod. 50 (4), 499–508.
Schrama, E., Wouters, B., 2011. Revisiting Greenland ice sheet mass loss observed by GRACE. J. Geophys. Res. 116, B02407.
Sørensen, L.S., Simonsen, S.B., Nielsen, K., Lucas-Picher, P., Spada, G., Adalgeirsdottir, G., Forsberg, R., Hvidberg, C.S., 2011. Mass balance of the Greenland ice sheet (2003–2008) from ICESat data—the impact of interpolation, sampling and firn density. Cryosphere 5 (4), 173–186.
Tamisiea, M.E., Mitrovica, J.X., Davis, J.L., 2007. GRACE gravity data constrain ancient ice geometries and continental dynamics over Laurentia. Science 316, 881–883.
Tapley, B., Bettadpur, S., Watkins, M., Reigber, C., 2004. The gravity recovery and climate experiment: mission overview and early results. Geophys. Res. Lett. 31 (9).
Thomas, R., Frederick, E., Krabill, W., Manizade, S., Martin, C., 2006. Progressive increase in ice loss from Greenland. Geophys. Res. Lett. 33 (L10503).
Tushingham, A.M., Peltier, W.R., 1992. Validation of the ICE-3G model of the Würm–Wisconsin deglaciation using a global data base of relative sea-level histories. J. Geophys. Res. 97, 3285–3304.
van den Broeke, M., Bamber, J., Ettema, J., Rignot, E., Schrama, E., van de Berg, W.J., van Meijgaard, E., Velicogna, I., Wouters, B., 2009. Partitioning recent Greenland mass loss. Science 326, 984–986.
Velicogna, I., 2009. Increasing rates of ice mass loss from the Greenland and Antarctic ice sheets revealed by GRACE. Geophys. Res. Lett. 36, L19503.
Velicogna, I., Wahr, J., 2005. Greenland mass balance from GRACE. Geophys. Res. Lett. 32 (18), L18505.
Velicogna, I., Wahr, J., 2006. Acceleration of Greenland ice mass loss in spring 2004. Nature 443, 329–331.
Wahr, J., Molenaar, M., Bryan, F., 1998. Time variability of the Earth's gravity field: hydrological and oceanic effects and their possible detection using GRACE. J. Geophys. Res. 103 (B12), 30205–30230.
Wolf, D., Klemann, V., Wünsch, J., Zhang, F.-P., 2004. A reanalysis and reinterpretation of geodetic and geomorphologic evidence of glacial-isostatic uplift in the Churchill region, Hudson Bay. Surv. Geophys. 27 (1), 19–61.
Zwally, H., Giovinetto, M., 2011. Overview and assessment of Antarctic ice-sheet mass balance estimates: 1992–2009. Surv. Geophys. 32 (4), 351–376.
Zwally, H., Schutz, R., Bentley, C., Bufton, J., Herring, T., Minster, J., Spinhirne, J., Thomas, R., 2010. GLAS/ICESat L2 Antarctic and Greenland Ice Sheet Altimetry Data V031. National Snow and Ice Data Center, Boulder, Colorado.
Zwally, H.J., Abdalati, W., Herring, T., Larson, K., Saba, J., Steffen, K., 2002. Surface melt-induced acceleration of Greenland ice-sheet flow. Science 297 (5579), 218–222.